



Neutral mononuclear and dinuclear complexes of gold(I) featuring azole ligands: Synthesis, structure and cytotoxicity

William F. Gabrielli^a, Stefan D. Nogai^a, Margo Nell^b, Stephanie Cronje^{a,c}, Helgard G. Raubenheimer^{a,*}

^a Department of Chemistry and Polymer Science, University of Stellenbosch, Private Bag X1, Matieland, 7602 Stellenbosch, South Africa

^b Department of Pharmacology, Prinshof Campus, University of Pretoria, P.O. Box 2034, Pretoria 0001, South Africa

^c Institut für Anorganische und Analytische Chemie, Goethe-Universität Frankfurt, Max-von-Laue-Strasse 7, D-60348 Frankfurt am Main, Germany

ARTICLE INFO

Article history:

Received 19 November 2011

Accepted 24 December 2011

Available online 4 January 2012

Keywords:

Azole

Gold complexes

Pentafluorophenyl

Cytotoxicity

HeLa cells

ABSTRACT

The aim of this work was to extend the small library of existing compounds of gold(I) that contain pentafluorophenyl and thiazole ligands and to determine the biological activity of such compounds against a well-known cancer cell line. Seven mono and dinuclear new compounds that contain imidazole, thiazole and tetrazole rings were isolated and characterised. Three of the crystal structures determined indicated Au...Au interactions between constituent complex molecules. A simple adduct, [Au(C₆F₅)(N-methylimidazole)], exhibits a relatively high anti-tumour specificity indicating the viability of selected phosphine-free gold complexes as cytotoxic agents.

© 2012 Elsevier Ltd. All rights reserved.

1. Introduction

The number of gold(I) complexes that contain nitrogen donors have steadily grown in recent years [1]. This class of complexes was recently expanded by description of the synthesis and characterisation of neutral azol-2-ylideneamine complexes containing C₆F₅, PPh₃ and (1,3-di-tert-butylimidazol-2-ylidene) as ancillary ligands [2]. A large number of neutral complexes based on azoles contain azolate ligands and they have been discussed in a previous article [3]. Phosphine complexes of gold(I) linked to neutral azoles are mostly of the cationic form [AuL(PPh₃)]⁺ (L = N-bonded azole) [4,5], although dicationic complexes with bidentate phosphine ligands, [Au₂L₂(μ-P[∧]P)]²⁺ (P[∧]P = ddpm, dppe, dppp) [6,7], are also known. Leonesi et al. [8] have prepared the first neutral azole complexes of gold(I) by substituting Me₂S from [AuCl(Me₂S)] with imidazole and substituted imidazoles. No definite structure have been assigned to the insoluble products but gold coordination numbers varying between two and three are proposed for the intermolecularly-associated compounds. A number of neutral azole complexes with empirical formula [AuX(L)] (L = substituted imidazole or oxazole; X = Cl or Br), have been prepared by Matović et al. [9] who, on the basis of vibrational spectra analyses, propose rather unlikely non-linear, halogen-bridged, dimeric structures in the solid state, which have not been confirmed by crystal and molecular structure determination. Cronje et al. [10], have more

recently unambiguously characterised neutral, linear, N-bonded gold(I) complexes of two substituted thiazole ligands with pentafluorophenyl as ancillary ligand.

The anti-proliferative, i.e. anti-viral, anti-bacterial, anti-fungal, anti-microbial, anti-cancer, anti-inflammatory and anti-infective, activity of gold(I) compounds and their clinical use in the treatment of severe of rheumatoid arthritis has provided a powerful incentive for the continued pursuit of the bonding of biologically active molecules to gold(I) and the investigation of their biological effects [11–13]. The coordination of biologically active molecules to metal centres has afforded compounds with amplified activity or therapeutic effect [14].

The development and investigation of the mechanisms of cytotoxicity and anti-tumour activity of gold(I) phosphine and carbene compounds has provided a new momentum in the search for new generations of chemotherapeutic agents [15,16].

Combination of nucleoside analogues with gold(I) might be beneficial in eliminating resistance and lowering toxicity. Azole-platinum compounds with comparable *in vitro* anticancer activity to cisplatin have shown improved cytotoxic activity in cell lines resistant to cisplatin [17]. A phosphine-free ‘complex of a complex’ consisting of a ferrocenyl moiety conjugatively part of an NHC ligand which is bound to gold(I), is tumour specific against the HeLa and Jurkat cancer cell lines. The question regarding possible antitumour activity enhancement by the presence of the ferrocenyl group remains unresolved, and needs to be further addressed [18]. Exocyclic imine complexation of azol-2-ylideneamine ligands with (Ph₃P)Au⁺ increases their antitumour as well as antimalarial activity [2].

* Corresponding author.

E-mail address: hgr@sun.ac.za (H.G. Raubenheimer).

Here we report the results of an investigation to prepare and characterise neutral pentafluorophenyl complexes of gold(I) that contain substituted neutral imidazoles, a bidentate ligand with thiazole units and, uniquely, a substituted tetrazole positioned in the second coordination position of the central metal(I) ion. Crystal structure determinations were carried out as well as a preliminary assay of the cytotoxicity of some of the new compounds to establish the biological activity of such phosphine-free complexes.

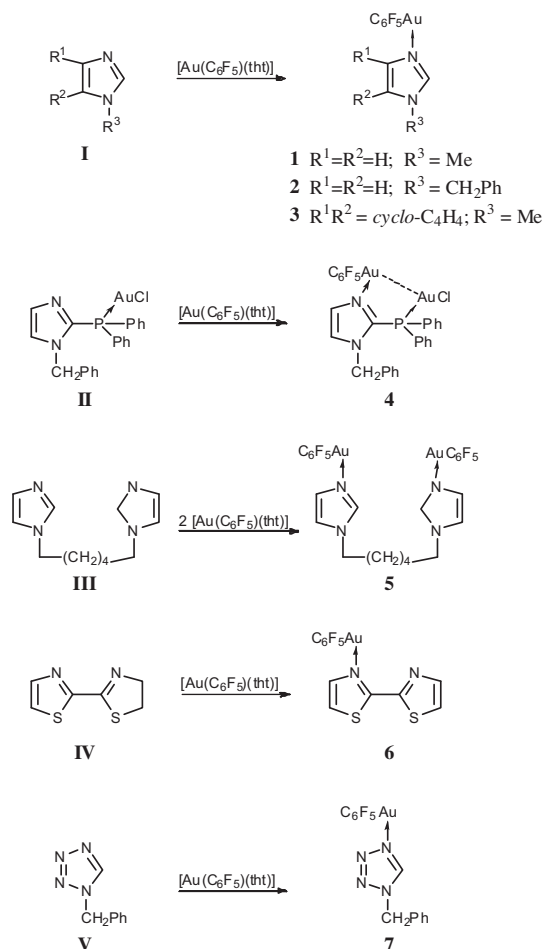
2. Results and discussion

2.1. Preparative studies

The neutral ligands **I–V** shown in Scheme 1 were coordinated to the C_6F_5Au -unit by simple substitution of labile tht (tht = tetrahydrothiophene) [19]. Compound **II**, that functions as a ligand, is a gold complex of derivatised benzyl imidazole and was prepared according to a method used by Burini et al. [20] while substituting $[AuCl(Me_2S)]$ rather than $[AuCl(tht)]$ that was used by them as starting material.

The complexes **1–5** were finally obtained as analytically pure crystals from solutions of dichloromethane (**1–4**) or tetrahydrofuran (**5**) layered with hexane at $-20^\circ C$.

X-ray quality crystals of **1–3** grew successfully, and the resultant structural determination by means of X-ray diffraction confirmed the molecular structures of these compounds. It is noteworthy that no homoleptically rearranged by-products of **1–3** in various solvents were identified during analysis in solution or in the solids.



Scheme 1.

Complex **5**, although stable at room temperature and under inert conditions for prolonged periods, is somewhat more air and moisture sensitive than **1–3**.

The microcrystalline complex **6** is insoluble in most polar and apolar organic solvents, and since characterisation by NMR was impossible, a molecular structure analysis by X-ray diffraction was crucial. In order to obtain crystals suitable for a crystal structure determination, we slowed down the reaction and thus the immediate formation of the microcrystalline product by working at lower temperature.

Whereas imine-coordination with imidazole substrates led to immediate product formation, the related tetrazole coordination required prolonged reaction periods and were incomplete. In this manner compound **7** was obtained as a colourless solid that is both air and moisture sensitive. Recrystallisation from dichloromethane layered with *n*-pentane at $-20^\circ C$ afforded colourless needles of the targeted complex and co-crystallised free ligand. These crystals were subjected to a crystal and molecular structure determination. Subsequent washing of the crystalline product with diethyl ether and stripping of solvent under vacuum, afforded **7** in pure form for further analysis and biological screening.

2.2. Characterisation

The 1H and ^{13}C NMR spectra for the compounds **1–3** and **5** provide limited information on the bonding in these complexes. The resonances of the atoms in the complexes are shifted consistently downfield ($\Delta\delta_H$ 0.3 and $\Delta\delta_C$ ca. 4.0) from their positions in the spectra of the free ligands. The most notable changes occur in the proton resonances of the acidic CH's (**2**), which show a more significant and consistent downfield shift of $\Delta\delta$ 1.0 upon coordination. High resolution ^{13}C and ^{19}F NMR spectra of these complexes confirm the presence of C_6F_5Au moieties in the noted distinctive C–F and F–F coupling patterns of the signals. Since no crystals of suitable dimension for crystal structure determination of **5** could be grown, we relied on elemental analysis and the pronounced ($\Delta\delta$ 52) upfield shift for the gold-coordinated nitrogen atoms (N^3) of the two imidazole rings compared to their signals in the free ligand, as evidence for dinuclear gold complex formation.

The chemical shifts of the dinuclear complex **4** can be compared to those for the parent complex **II** with all the spectra measured in CD_2Cl_2 . The broadened, incompletely resolved 1H NMR signal for the CH_2 unit can be ascribed to H–P coupling across (alkylated) N^1 , in contrast to the sharp singlet found for the same proton in **II**. The two distinct sets of doublets of doublets – both integrating for single protons and representing two chemically non-equivalent nuclei, are assigned to protons H^4 and H^5 . Apart from the $^3J_{HH}$ coupling of 7.2 and 7.8 Hz, long range $^4J_{HP}$ coupling of 1.6 and 1.9 Hz across the nitrogen atom was noted, for H^4 and H^5 , respectively. Similar coupling patterns cannot be observed in complex **II** due to overlap with the aromatic signals. No conclusion could thus be drawn on whether complexation at N^3 , favours longer range coupling of the allylic protons to the phosphorus atom or not. The ^{13}C NMR spectrum of **4** shows distinctive C–P coupling patterns for the chemically non-equivalent phenyl carbons and diagnostic C^2 carbon. The azole carbon in the 2-position appears as a doublet, with an insignificant upfield shift ($\Delta\delta$ 1.3) compared to the corresponding complex–ligand **II**. The characteristic and complicated C–F coupling patterns were partly (because of overlap with aromatic signals) assigned to the pentafluorophenyl moiety. The most apparent difference is noted in the ^{31}P NMR singlet resonance in **4** which experiences a downfield shift of 6.54 ppm (to δ 17.24) relative to complex **II**.

A pronounced downfield shift ($\Delta\delta$ 49) of the resonance for coordinated N^4 in the ^{15}N NMR [$^1H, ^{15}N$ gHMQC] spectrum of **7** compared to that of free 1-benzyltetrazole, provides unambiguous

evidence for the coordination of a gold(I) centre to this nitrogen atom.

Molecular ions of **1** (m/z 446), **2** (m/z 522), **3** (m/z 496), **6** (m/z 588) and **7** (m/z 524) are observed in the electron impact mass spectra, whereas the molecular ion peaks of **4** (m/z 938; ^{35}Cl) and **5** (m/z 918) were only obtained by the softer FAB ionisation. Diagnostic fragmentations for **4** include the loss of AuCl (m/z 706) and loss of $\text{C}_6\text{F}_5\text{Au}$ (m/z 574) from the molecular ion.

A conspicuous omission from the fragmentation pattern of the imine complex **7** is the initial loss of dinitrogen that is characteristic in the ionisation of free 1- and 5-substituted tetrazoles, 1-benzyltetrazol-2-yl(diphenyl)phosphines and gold(I) complexes thereof, various tetrazol-5-ylidene-gold(I) complexes and trialkyl-phosphine(tetrazol-1-yl)gold(I) complexes [21]. The N^4 -imine coordination to gold(I) appears to stabilise the ring against the fragmentation prevalent in this class of compounds.

2.3. X-ray structure determination

The crystal and molecular structures of compounds were determined by single crystal X-ray diffraction. Their molecular structures and selected bond lengths and bond angles are depicted in Figs. 1–6. Although compounds **4** and **6** that differ from the rest in having somewhat more complicated ligands or structures exhibit seemingly somewhat longer Au–N separations and respectively somewhat shorter and longer Au–C distances, these elongations and shortenings remain within 4σ .

The neutral molecules in complex **1** are paired in the crystal lattice by weak hydrogen bonds involving the acidic azole hydrogen and a phenyl fluorine atom. It is striking that no intermolecular aurophilic interactions occur in this rather simple gold(I) complex derived from non-bulky ligands especially considering the remarkable stability of the complex in crystalline form.

The molecular structure of **2** (Fig. 2) can be described as two discrete linear two-coordinate molecules, which assemble in the unit cell as dimeric units. Weak aurophilic interactions between the gold centres [Au(1)–Au(2) 3.2237(3) Å] are attained by a staggered conformation about the metallic bond plane. This places the planes through the pentafluorophenyl substituents parallel to one another, whilst the planes through the imidazole rings appear at an angle.

The linear complex **3**, depicted in Fig. 3, is involved in aurophilic interaction [Au...Au at 3.2896(3) Å] with a neighbouring molecule across an inversion centre, and the two complexes ap-

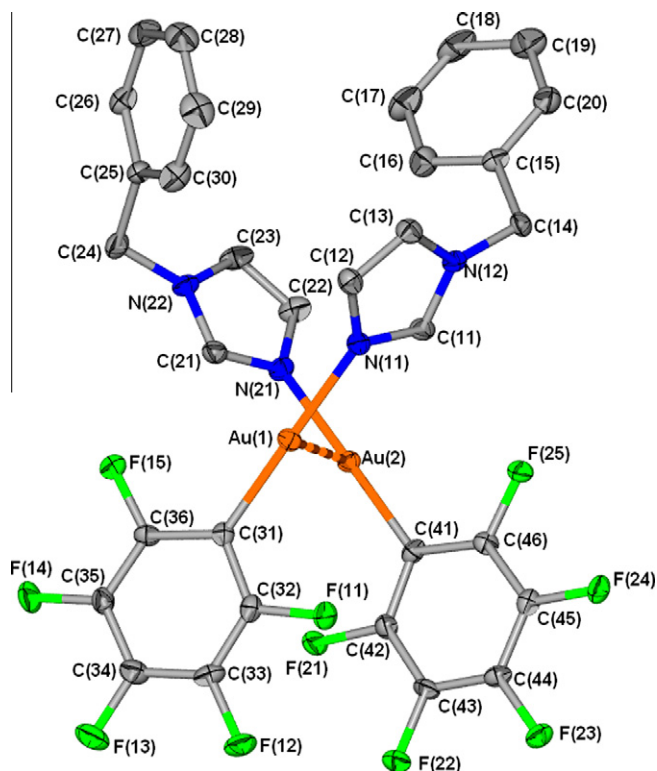


Fig. 2. Molecular structure of **2** showing the numbering scheme. Bond lengths: Au(1)–C(31) 1.996(5) Å, Au(1)–N(11) 2.049(4) Å, Au(1)–Au(2) 3.2237(3) Å; bond angles: C(31)–Au(1)–N(11) 179.0(2)°, C(41)–Au(2)–N(21) 177.6(6)°.

proach each other in a head to toe fashion. In addition, the C_6F_5 and imine substituents are co-planar and as a result of weak π -stacking interaction between pentafluorophenyl and the 5-membered ring of benzimidazole (distance between centroids 3.484 Å) of the paired units, allow efficient packing in the crystal lattice.

The molecular structure of complex **4** is given in Fig. 4. The colourless complex crystallises together with one mole quantity of dichloromethane in the triclinic space group $P\bar{1}$.

The neutral binuclear structure shows the two metal centres bridged by a BzimPPh₂ (Bzim = benzimidazole) ligand, with Au(1) coordinated to the phosphorus atom and Au(2) to the imine-N

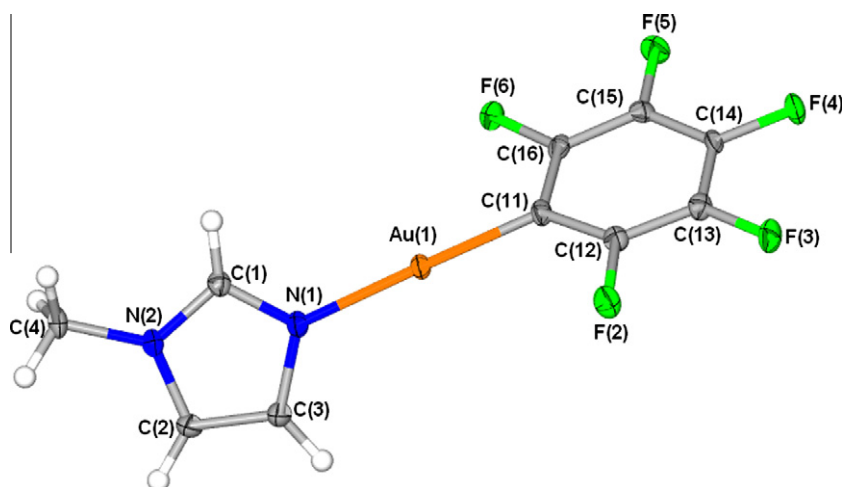


Fig. 1. Molecular structure of **1** showing the numbering scheme with 50% probability ellipsoids. Bond lengths: Au(1)–C(11) 2.001(4) Å, Au(1)–N(1) 2.044(3) Å; bond angle: C(11)–Au(1)–N(1) 177.1(1)°.

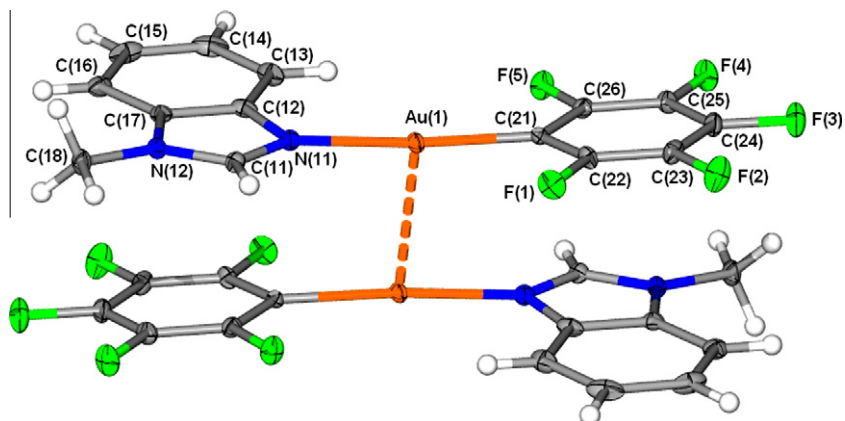


Fig. 3. Molecular structure of **3** showing the numbering scheme. Bond lengths: Au(1)–C(21) 2.008(4) Å, Au(1)–N(11) 2.046(3) Å, Au(1)–Au(1) 3.2896(3) Å; bond angles: C(21)–Au(1)–N(11) 175.6(1)°, C(21)–Au(1)–Au(1) 98.1(1)°.

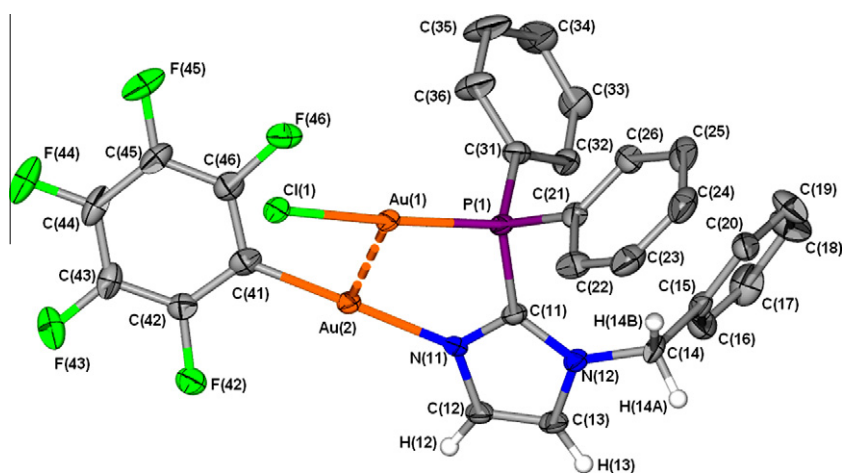


Fig. 4. Molecular structure of **4** showing the numbering scheme; phenyl hydrogens and unlinked solvent (dichloromethane) omitted. Bond lengths: Au(1)–P(1) 2.228(2), Au(1)–Cl(1) 2.290(1) Å, Au(2)–C(41) 1.986(7) Å, Au(2)–N(11) 2.060(5) Å, Au(1)–Au(1) 3.0079(5) Å; bond angles: P(1)–Au(1)–Cl(1) 174.15(6)°, C(41)–Au(2)–N(11) 179.0(2)°.

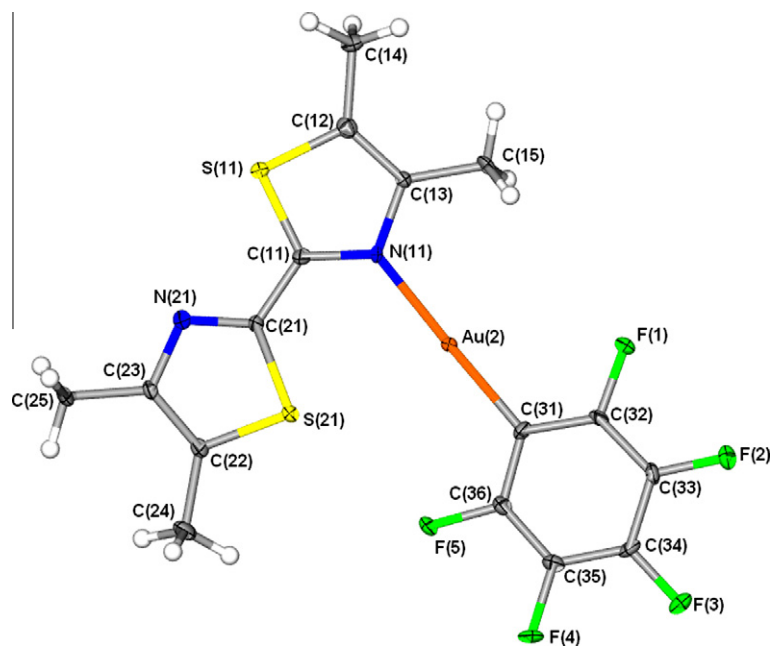


Fig. 5. Molecular structure of **6** showing the numbering scheme. Bond lengths: Au(2)–C(31) 2.014(7) Å, Au(2)–N(11) 2.061(6) Å; bond angle: C(31)–Au(2)–N(11) 178.4(2)°.

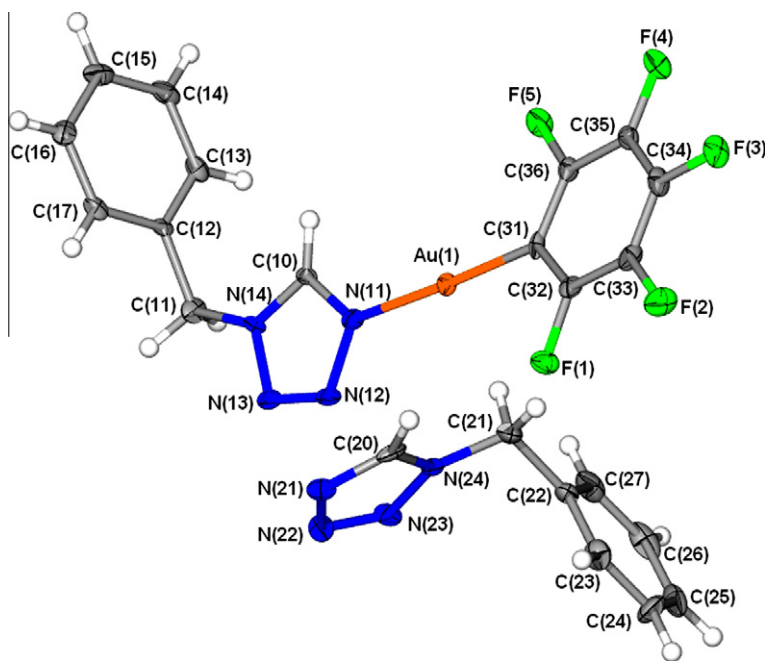


Fig. 6. Molecular structure of 7-benzyltetrazole showing the numbering scheme and the presence of a free ligand in the unit cell. Bond lengths: Au(1)–C(31) 2.004(6) Å, Au(1)–N(11) 2.050(5) Å; bond angle: C(31)–Au(1)–N(11) 177.5(2)°.

(N11) on the imidazole ring. Compared to the linear C(41)–Au(2)–N(II) angle, some distortion from linearity occurs in P1–Au(1)–Cl(1) [174.15(6)°].

The relatively short intramolecular aurophilic separation of 3.0079(5) Å is similar to the intramolecular metal contacts in the related dibridged compound [(AuCl)₂{(Ph₂P)₂CH₂}₂] [2.962(1) Å] [22] and in the tetranuclear complex, [Au{S=CNC(CH₃)=CHS}]₄ [3.02(4) Å] [10]. The two centres of coordination, Cl–Au–P and C–Au–N, are crossed, with the resultant plane of the five membered metallocyclic ring twisted by about 30° from planarity, [torsion angles Au(1)–P(1)–C(11)–N(11) and Au(1)–Au(2)–N(11)–C(11) at 35.7(6)° and –26.6(5)°, respectively]. In contrast, the cationic complex [Au₂(imPPPh₂)₂]²⁺ (im = imidazole) shows almost perfect planarity [23]. Dichloromethane solvent molecules are dispersed along each of the regularly packed rows of molecules.

Compound **6** (Fig. 5) crystallises in the triclinic space group *P* $\bar{1}$ as yellowish needles. The planes of the two thiazole rings that constitute the ligand are almost co-planar [torsion angles N(11)–C(11)–C(21)–N(21) and S(11)–C(11)–C(21)–N(21) at 171.5(7) and –8.6(9), respectively]. The bond lengths in the coordinated ring [N(11)–C(11) 1.329(9) Å and N(11)–C(13) 1.408(9) Å] remain largely unchanged compared with bond lengths in the uncoordinated ring [N(21)–C(21) 1.321(9) Å and N(21)–C(23) 1.375(9) Å].

Possible electron charge delocalisation from N(21) effected by gold(I) coordination to N(11) that could rationalise the mono-substitution, remains unsubstantiated, owing to typical single bond character of C(21)–C(11) [1.447(10) Å]. Molecules in the crystal lattice are organised in closely knitted sheets in the *bc* plane that stack upon one another along the *a*-axis by translation. Molecules arrange across the gold centres, with C₆F₅ moieties in a *trans* configuration about the coordinative axis of adjacent molecules. The structure is devoid of sulfur–Au(I) or aurophilic interactions. Intermolecular interactions are limited to π -stacking between the thiazole and pentafluorophenyl ring (distance between centroids 3.554 Å), which brings the non-interactive gold(I) centres in the closest possible separation at 3.679 Å.

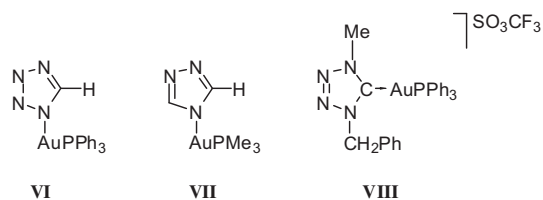
The molecular structure of **7** (Fig. 6) that co-crystallises with a molecule of free ligand (1-benzyltetrazole) in the monoclinic space group *P*2₁/*c*, can best be described as a discrete monomer consist-

ing of a C₆F₅Au unit, coordinated to a neutral imine within tetrazole while creating an almost linear geometry about the gold(I) atom. Of the three unsubstituted nitrogen atoms, only N(14) (N⁴ in the NMR discussion) is involved in coordination to the gold centre. It is worth mentioning that the Au(1)–N(11) [2.050(5) Å], adjacent N(11)–N(12) [1.368(7) Å] and C(10)–N(11) [1.310(7) Å] bond distances in the tetrazole imine complex are consistent with Au–N [2.043(5) Å], N–N [1.336(6) Å] and C–N [1.306(7) Å] bond lengths in the related triphenylphosphine(tetrazol-1-yl)gold(I) amine complex (the only entry of a ring substituted tetrazole complex of gold in the Cambridge Crystallographic database) [24]. The free ligand guest in the unit cell associates with the gold(I) complex through weak fluorine and hydrogen interactions. Apart from additional fluorine–hydrogen interaction, π -stacking interactions of the phenyl rings govern the lattice organisation.

2.4. Cytotoxicity studies

Cytotoxicity assays are performed to establish the sensitivity of cancer cell lines and normal cell cultures to selected compounds. In a standard procedure, a known concentration of cells is exposed to different concentrations of the experimental drug in a 96 well tissue culture plate and incubated for a selected period of time. Incubation periods can range from three to 7 days. The results obtained in such experiments enable the calculation of the concentration of the experimental compound that inhibits 50% of growth (IC₅₀). This method is applicable to both cancer cells and lymphocytes. From such results a coarse tumour specificity can be calculated, i.e. (mean IC₅₀ of healthy lymphocytes)/(mean IC₅₀ of the cancer cells).

The *in vitro* cytotoxic potency of altogether five compounds as well as cisplatin serving as benchmark were evaluated by determining their activity using cervical carcinoma cells (HeLa; ATCC CCL-2) as the target cell line. Compounds **1** and **7** are neutral azolyl (pentafluorophenyl)gold(I), complexes whereas the structures of **VI** [25], **VII** (see Section 4 for preparative details) and **VIII** [21c] that all contain a cationic gold phosphine unit attached to different N-heterocyclic ring systems, are shown in Scheme 2. To evaluate whether any cytotoxicity observed against HeLa cells could not be tumour specific, additional dose–response assays were performed to derive



Scheme 2.

Table 1
Cytotoxicity ($IC_{50}^{a,b}$) of cisplatin and gold complexes against HeLa cells and human lymphocytes.

Compound	HeLa	Human lymphocytes (resting)	Human lymphocytes (PHA stimulated)
1	0.55 (0.09)	8.37 (0.96)	8.18 (1.75)
7	1.39 (0.16)	–	–
VI	1.27 (0.72)	2.58 (0.01)	2.45 (1.29)
VII	2.33 (0.14)	–	–
VIII	1.67 (0.20)	–	–
Cisplatin	0.45 (0.12)	48.71 (1.82)	2.88 (1.17)

^a Mean drug concentration $\mu\text{mol/l}$ (standard deviation in brackets) causing 50% cell death under chosen conditions.

^b Average of not less than three independent experiments.

IC_{50} values against normal, resting and phytohaemagglutinin (PHA)-stimulated human lymphocytes for the two compounds, **1** and **VI**, that exhibited the lowest IC_{50} s against HeLa cells. The results for the cytotoxicity assays are reported in Table 1.

From the results it is clear that the relatively simple neutral complex **1** performs much better against cervical carcinoma cells (HeLa; ATCC CCL-2) than the phosphine-free tetrazolate complex **7** or the phosphine complexes **VII** and **VIII**. The phosphine (tetrazolate) complex **VI** probably has a similar potency to the latter three but, unfortunately, its results show a larger variability. The imidazole(pentafluorophenyl)gold(I) complex, **1**, effects a tumour specificity [$IC_{50}(\text{av. lymph})/IC_{50}(\text{HeLa})$] of 15 compared to 2.0 for **VI** and 57 for cisplatin. We established, however [3b], that all these mononuclear compounds exhibit much lower cytotoxicity than dinuclear azolate-type gold compounds of diphosphines with carbon chain lengths of 5 and 6 between the two phosphorous atoms – even when normalised with respect to the mole quantities gold and phosphorous that they contain. It could, in the light of the present results, prove worthwhile to investigate related dinuclear complexes with neutral azoles as ligands, particularly phosphine-free analogues. The carbene ligands developed by Baker and co-workers [26] could be ideally suited for such a purpose.

3. Conclusion

The small number of well-characterised neutral gold complexes that contain imine-bonded azoles, has been extended by the preparation and crystal structure determination of a number of very stable complexes based on substituted imidazole, thiazole and tetrazole. The simplest complex now prepared, $[\text{Au}(\text{C}_6\text{F}_5)(\text{N-methylimidazole})]$, shows no aurophilic interaction in the solid state whereas three other complexes crystallizes with one or other form gold–gold interaction present. Our investigation clearly indicates, first, that phosphine auxiliary ligands in certain gold(I) complexes can be replaced by the pentafluorophenyl anion without loss of cytotoxicity and, secondly, that neutral azoles should be included in the list of viable ligands for biological activity studies.

4. Experimental

4.1. Materials and physical measurements

Reactions were carried out under argon using standard Schlenk and vacuum-line techniques. Tetrahydrofuran (thf), *n*-hexane, *n*-pentane and diethyl ether were distilled under N_2 from sodium benzophenone ketyl, dichloromethane and *N,N'*-dimethylformamide (DMF) from CaH_2 , ethanol and methanol from magnesium. 1-Methylimidazole, 1-benzylimidazole, sodium azide and ammonium chloride were purchased from Aldrich. Butyllithium (1.6 M solution *n*-hexane), sodium hydride, dimethyldisulfide, triethyl orthoformate and glacial acetic acid were purchased from Merck. Literature methods were followed to prepare 1-benzyltetrazole [27], 1-methylbenzimidazole [28] 1,4-bis(imidazol-1-yl)butane [29], 1,2-di(tetrazol-2-yl)ethane [30], 2,2'-bis(4,5-dimethylthiazole) [31], $[\text{AuCl}(\text{tht})]$ [32], $[\text{Au}(\text{C}_6\text{F}_5)(\text{tht})]$ [33], and chloro[(1-benzylimidazol-2-yl)diphenyl]phosphinegold(I) [30].

Melting points were determined on a Stuart SMP3 apparatus and are uncorrected. Mass spectra were recorded on an AMD 604 (EI, 70 eV), VG Quattro (ESI, 70 eV methanol, acetonitrile) or VG 70 SEQ (FAB, 70 eV) instruments. In the EI and FAB MS results the isotopic distribution patterns confirmed the theoretical distribution. All NMR spectra were recorded on a Varian 300 FT or INOVA 600 MHz spectrometer (^1H NMR at 300/600 MHz, $^{13}\text{C}\{^1\text{H}\}$ NMR at 75/150 MHz, $^{31}\text{P}\{^1\text{H}\}$ NMR at 121/243 MHz, ^{15}N NMR at 60.8 MHz and ^{19}F NMR at 376 MHz). Chemical shift (δ) is reported relative to solvent resonance or external reference of 85% H_3PO_4 (^{31}P), NH_3NO_2 (^{15}N) and CFCl_3 (^{19}F). Infrared spectra were recorded on a Thermo Nicolet Avatar 330FT-IR with Smart OMNI ATR (attenuated total reflectance) sampler. Elemental analysis was carried out at the School of Chemistry, University of the Witwatersrand. For elemental analysis, products were evacuated under high vacuum for 10 h.

4.2. Preparation of 1-methylimidazole(pentafluorophenyl)gold(I) (**1**)

The addition of a solution of 1-methylimidazole (0.17 g, 2.1 mmol) in diethyl ether (20 ml) to a solution of freshly prepared $[\text{Au}(\text{C}_6\text{F}_5)(\text{tht})]$ (0.95 g, 2.1 mmol) in diethyl ether (20 ml) produced a cloudy solution. The mixture was stirred for 1.5 h at room temperature upon which the solution was reduced to dryness *in vacuo*. The white residue was extracted with diethyl ether, filtered through anhydrous MgSO_4 and the filtrate concentrated *in vacuo* to yield a white microcrystalline material. Recrystallisation of the white solid by layering a dichloromethane solution with *n*-hexane produced colourless needles, **1** (0.70 g) at -20°C .

Yield: 75%. Mp 136°C . EI-MS, m/z (relative intensity) for $\text{C}_{10}\text{H}_6\text{AuF}_5\text{N}_2$: 446 (M^+ , 9), 364 (AuC_6F_5^+ , 2), 334 ($\text{C}_{12}\text{F}_{10}^+$, 100), 279 ($\text{M}^+ - \text{C}_6\text{F}_5$, 5), 265 ($\text{C}_{11}\text{F}_7^+$, 36), 82 ($\text{M}^+ - \text{AuC}_6\text{F}_5$, 28). ^1H NMR (300 MHz, CD_2Cl_2 , δ_{H}) 3.77 (s, 3H, NCH_3), 7.13 (m, 1H, CHN^1), 7.15 (m, 1H, CHN^3), 7.78 (s, 1H, $\text{NC}(\text{H})\text{N}$). ^{13}C NMR (75 MHz, CD_2Cl_2 , δ_{C}) 35.1 (s, NCH_3), 117.9 (tm, $J_{\text{CF}} = 56.4$ Hz, *ipso*- C_6F_5), 121.7 (s, CHN^1), 129.5 (s, CHN^3), 137.1 (dm, $J_{\text{CF}} = 249.9$ Hz, *meta*- C_6F_5), 138.8 (dm, $J_{\text{CF}} = 245.3$ Hz, *para*- C_6F_5), 139.4 (s, $\text{NC}(\text{H})\text{N}$), 149.9 (ddm, $J_{\text{CF}} = 228.0$ Hz, $J_{\text{CF}} = 24.2$ Hz, *ortho*- C_6F_5). ^{15}N NMR (61 MHz, CD_2Cl_2 , δ_{N}) -217.7 (s, $\text{N}1$), -166.3 (s, $\text{N}3$). Anal. Calc. for $\text{C}_{10}\text{H}_6\text{AuF}_5\text{N}_2$ (446.13): C, 26.92; H, 1.36; N, 6.28. Found: C, 26.58; H, 1.41; N, 6.22%.

4.3. Preparation of 1-benzylimidazole(pentafluorophenyl)gold(I) (**2**)

This product was prepared in a similar fashion as **1** from 1-benzylimidazole (0.04 g, 0.3 mmol) and $[\text{Au}(\text{C}_6\text{F}_5)(\text{tht})]$ (0.12 g,

Table 2
Crystallographic data.

	1	2
Empirical formula	C ₁₀ H ₆ F ₅ N ₂ Au	C ₁₆ H ₁₀ AuF ₅ N ₂
M _r	446.13	522.23
T (K)	100(2)	100(2)
λ (Å)	0.71073	0.71073
Crystal system	triclinic	triclinic
Space group	P $\bar{1}$	P $\bar{1}$
a (Å)	4.7900(3)	8.1714(8)
b (Å)	10.3738(6)	13.4065(13)
c (Å)	11.0755(7)	14.5984(13)
α (°)	88.0840(10)	77.470(2)
β (°)	86.0360(10)	86.845(2)
γ (°)	82.6480(10)	79.489(2)
V (Å ³)	544.35(6)	1534.8(3)
Z	2	4
D _{calc} (g cm ⁻³)	2.722	2.260
Absorption coefficient (μ, mm ⁻¹)	13.563	9.640
Absorption correction	semi-empirical from equivalents	semi-empirical from equivalents
F(000)	408	976
Crystal size (mm)	0.30 × 0.20 × 0.20	0.30 × 0.20 × 0.15
θ-range for data collection (°)	1.84–28.24	1.89–25.68
Index range	–6 ≤ h ≤ 6 –13 ≤ k ≤ 13 –14 ≤ l ≤ 14	–9 ≤ h ≤ 9 –16 ≤ k ≤ 15 –10 ≤ l ≤ 17
Number of reflections collected	6256	8529
Number of independent reflections	2494 (R _{int} = 0.0235)	5710 (R _{int} = 0.0176)
Maximum and minimum transmission	0.2355 and 0.1318	0.3258 and 0.2133
Refinement method	Full-matrix least-squares on F ²	Full-matrix least-squares on F ²
Data/restraints/parameters	2494/0/165	5710/0/433
Gof on F ²	1.056	1.025
Final R-indices [I > 2σ > (I)]	R ₁ = 0.0194 wR ₂ = 0.0444	R ₁ = 0.0263 wR ₂ = 0.0635
R indices (all data)	R ₁ = 0.0209 wR ₂ = 0.0451	R ₁ = 0.0308 wR ₂ = 0.0656
Largest difference in peak and hole (e Å ⁻³)	1.487 and –0.566	1.952 and –0.641
Weighing scheme	a = 0.0221/b = 0.2729	a = 0.0384

0.27 mmol). Colourless crystals of **2** (0.11 g) were obtained, from a dichloromethane solution layered with *n*-hexane, at –20 °C.

Yield: 75%. Mp: 120–122 °C. EI-MS, *m/z* (relative intensity) for C₁₆H₁₀AuF₅N₂: 522 (M⁺, 25), 364 (AuC₆F₅⁺, 6), 334 (C₁₂F₁₀⁺, 62), 355 (M⁺–C₆F₅, 2), 265 (C₁₁F₇⁺, 22), 158 (M⁺–AuC₆F₅, 100). ¹H NMR [600 MHz, (CD₃)₂CO, δ_H] 5.47 (bs, 2H, CH₂Ph), 7.29 (m, 1H, CHN³), 7.36–7.45 (m, 5H, –CH₂C₆H₅), 7.60 (m, 1H, CHN¹), 8.46 (m, 1H, NC(H)N). ³¹C NMR [150 MHz, (CD₃)₂CO, δ_C] 53.4 (s, NCH₂), 119.2 (tm, J_{CF} = 54.1 Hz, *ipso*-C₆F₅), 122.9 (s, CHN¹), 129.4 (s, *ipso*-C₆H₅CH₂), 129.9 (s, *meta*-C₆H₅CH₂), 130.4 (s, *para*-C₆H₅CH₂), 130.7 (s, CHN³), 130.9 (s, *ortho*-C₆H₅CH₂), 135.3 (dm, J_{CF} = 251.4 Hz, *meta*-C₆F₅), 139.4 (dm, J_{CF} = 243.6 Hz, *para*-C₆F₅), 141.5 (s, NC(H)N), 150.3 (ddm, J_{CF} = 227.2 Hz, J_{CF} = 24.2 Hz, *ortho*-C₆F₅). ¹⁹F NMR [376 MHz, (CD₃)₂CO, δ_F] –115.7 (m, 2F, *ortho*-F), –161.7 (t, J_{FF} = 19.5 Hz, 2F, *meta*-F), –164.3 (m, F, *para*-F). Anal. Calc. for C₁₆H₁₀AuF₅N₂ (522.23): C, 36.80; H, 1.93; N, 5.36. Found: C, 36.91; H, 1.90; N, 5.71%.

4.4. Preparation of 1-methylbenzimidazole(pentafluorophenyl)gold(I) (**3**)

This product was prepared in a similar manner as **1** from 1-methylbenzimidazole (0.04 g, 0.3 mmol) and [Au(C₆F₅)(tht)] (0.12 g, 0.27 mmol). Colourless crystals of **3** (0.09 g) were obtained, from a dichloromethane solution layered with *n*-hexane, at –20 °C.

Yield: 71%. Mp: 233 °C (decomp.). EI-MS, *m/z* (relative intensity) for C₁₄H₈AuF₅N₂: 496 (M⁺, 2), 334 (C₁₂F₁₀⁺, 100), 265 (C₁₁F₇⁺, 55), 132 (M⁺–AuC₆F₅, 100). ¹H NMR [300 MHz, (CD₃)₂CO, δ_H] 4.15 (s, 3H, NCH₃), 7.53 (m, 2H, *ortho*-C₆H₄), 7.96 (m, 1H, *meta*-C₆H₄) and 7.83 (m, 1H, *meta*-C₆H₄), 8.82 (s, 1H, NC(H)N). ³¹C NMR [75 MHz, (CD₃)₂CO, δ_C] 33.6 (s, NCH₃), 113.8/120.1 (s, *ortho*-C₆H₄), 126.4/127.2 (s, *meta*-C₆H₄), 117.7 (m, *ipso*-C₆F₅), 135.6 (s, CHN¹), 138.7

(dm, J_{CF} = 242.8 Hz, *meta*-C₆F₅), 140.4 (dm, J_{CF} = 244.5 Hz, *para*-C₆F₅), 142.4 (s, CHN³), 148.6 (s, NC(H)N), 151.7 (ddm, J_{CF} = 227.6 Hz, J_{CF} = 24.1 Hz, *ortho*-C₆F₅). ¹⁹F NMR [376 MHz, (CD₃)₂CO, δ_F] –115.8 (m, 2F, *ortho*-F), –157.1 (t, J_{FF} = 19.3 Hz, 2F, *meta*-F), –161.3 (m, F, *para*-C₆F₅). Anal. Calc. for C₁₄H₈AuF₅N₂ (496.19): C, 33.89; H, 1.63; N, 5.65. Found: C, 33.60; H, 1.51; N, 5.82%.

4.5. Preparation of chloro[1-benzyl-N-pentafluorophenylgold(I)imidazol-2-yl](diphenyl)phosphinegold(I) (**4**)

A solution of chloro[(1-benzylimidazol-2-yl)diphenyl]phosphinegold(I) (0.13 g, 0.22 mmol) in diethyl ether/thf (10:1, 20 ml) was treated with a solution of freshly prepared [Au(C₆F₅)(tht)] (0.10 g, 0.22 mmol) in diethyl ether (20 ml). The clear solution was stirred at room for 48 h temperature. The resultant cloudy solution was reduced to dryness under vacuum. The off-white oily residue was repeatedly washed with *n*-hexane to afford a white solid. Recrystallisation by layering a dichloromethane solution with *n*-hexane afforded colourless, crystalline material, **4** (0.15 g,) at –20 °C.

Yield: 73%. Mp: 117 °C (decomp.). EI-MS, *m/z* (relative intensity) for C₂₈H₁₉N₂F₅ClPAu₂: 938 (M³⁵Cl⁺, 100), 741 (M⁺–Au, 1), 706 (M⁺–AuCl, 16), 574 (M⁺–AuC₆F₅, 12), 342 (BzimPPH₂⁺, 70). ¹H NMR (300 MHz, CD₂Cl₂, δ_H) 5.30 (bs, 2H, CH₂Ph), 6.83 (dd, 1H, ³J = 7.2 Hz, ⁴J_{HP} = 1.6 Hz, CHN³), 7.23 (dd, 1H, ³J = 7.8 Hz, ⁴J_{HP} = 1.9 Hz, CHN¹), 7.18–7.44 (m, 5H, –CH₂C₆H₅), 7.42–7.72 (m, 10H, P(C₆H₅)₂). ³¹C NMR (75 MHz, CD₂Cl₂, δ_C) 53.3 (s, CH₂Ph), 117.7 (m, *ipso*-C₆F₅), 124.8 (d, ¹J_{CP} = 65.3 Hz, *ipso*-C₆H₅P), 127.0–135.0 (m, *para*-C₆F₅), 127.0–135.0 (m, *meta*-C₆F₅), 127.7 (s, CHN¹), 128.1 (s, *ipso*-C₆H₅CH₂), 129.4 (s, *m*-C₆H₅CH₂), 129.8 (s, CHN³), 130.5 (d, ³J_{CP} = 12.7 Hz, *meta*-P(C₆H₅)₂), 133.0 (s,

Table 3
Crystallographic data.

	3	4-CH₂Cl₂
Empirical formula	C ₁₄ H ₈ AuF ₅ N ₂	C ₄₃ H ₂₃ F ₅ N ₂ Cl ₂ PAu ₂
M _r	496.19	1158.47
T (K)	100(2)	100(2)
λ (Å)	0.71073	0.71073
Crystal system	monoclinic	triclinic
Space group	P2 ₁ /c	P $\bar{1}$
a (Å)	11.0548(11)	10.505(2)
b (Å)	8.1204(8)	12.697(2)
c (Å)	15.1295(16)	13.241(2)
α (°)	90	113.914(3)
β (°)	101.383(2)	103.872(2)
γ (°)	90	90.991(3)
V (Å ³)	1331.5(2)	1554.2(4)
Z	4	2
D _{calc} (g cm ⁻³)	2.475	2.187
Absorption coefficient (μ, mm ⁻¹)	11.104	9.791
Absorption correction	semi-empirical from equivalents	semi-empirical from equivalents (SADABS)
F(000)	920	956
Crystal size (mm)	0.20 × 0.20 × 0.10	0.20 × 0.10 × 0.10
θ-range for data collection (°)	1.88–26.37	1.75–26.73
Index range	–11 ≤ h ≤ 13 –10 ≤ k ≤ 9 –18 ≤ l ≤ 15	–7 ≤ h ≤ 13 –13 ≤ k ≤ 16 –16 ≤ l ≤ 16
Number of reflections collected	7396	9244
Number of independent reflections	2707 (R _{int} = 0.0220)	6419 (R _{int} = 0.0146)
Maximum and minimum transmission	0.4031 and 0.2039	0.3749 and 0.2408
Refinement method	Full-matrix least-squares on F ²	Full-matrix least-squares on F ²
Data/restraints/parameters	2707/0/200	6419/0/379
Gof on F ²	1.059	1.104
Final R-indices [I > 2σ > (I)]	R ₁ = 0.0221 wR ₂ = 0.0520	R ₁ = 0.0350 wR ₂ = 0.0837
R indices (all data)	R ₁ = 0.0244 wR ₂ = 0.0531	R ₁ = 0.0400 wR ₂ = 0.0860
Largest difference in peak and hole (e Å ⁻³)	1.557 and –1.283	2.140 and –1.464
Weighing scheme	a = 0.0312/b = 0.9283	a = 0.0360/b = 11.0208

para-P(C₆H₅)₂, 133.4 (d, ¹J_{CP} = 63.1 Hz, NC(P)N), 133.4 (s, *para*-C₆H₅CH₂), 134.8 (d, ²J_{CP} = 14.8 Hz, *ortho*-P(C₆H₅)₂), 141.2 (s, *ortho*-C₆H₅CH₂), 149.6 (ddm, J_{CF} = 231.0, J_{CF} = 28.0 Hz, *ortho*-C₆F₅). ³¹P NMR (121 MHz, CD₂Cl₂, δ_P) 17.24 (s). ¹⁹F NMR (376 MHz, CD₂Cl₂, δ_F) –114.7 (m, 2F, *ortho*-F), –161.4 (t, J = 21.3 Hz, F, *para*-F) and –162.7 (m, 2F, *meta*-F). Anal. Calc. for C₂₈H₁₉N₂F₅ClPAu₂ (938.82): C, 35.82; H, 2.04; N, 2.98. Found: C, 36.10; H, 2.22; N, 3.14%.

4.6. Preparation of [1,4-bis(imidazol-1-yl)butane]bis(pentafluorophenyl)gold(I) (**5**)

This product was prepared in a similar fashion as **1** from 1,4-bis(imidazol-1-yl)butane (0.05 g, 0.3 mmol) in methanol (10 ml) and [Au(C₆F₅)(tht)] (0.23 g, 0.50 mmol) in thf/methanol (10:1, 10 ml). Colourless microcrystalline material of **5** (0.19 g) was obtained, from a thf solution layered with *n*-hexane, at –20 °C.

Yield: 83%. Mp: 148 °C (decomp.). EI-MS, *m/z* (relative intensity) for C₂₂H₁₄N₄F₁₀Au₂: 918 (M⁺, 2), 751 (M⁺–C₆F₅, 13), 555 (M⁺–AuC₆F₅, 12), 387 (M⁺–Au(C₆F₅)₂, 12), 191 (M⁺–[Au(C₆F₅)₂], 15). ¹H NMR [600 MHz, (CD₃)₂SO, δ_H] 1.75 (q, 4H, ³J = 2.8 Hz, NCH₂CH₂), 4.12 (t, 4H, ³J = 5.0 Hz, NCH₂), 7.29 (dd, 2H, ³J = 2.8 Hz, ⁴J = 0.4 Hz, CHN³), 7.64 (dd, 2H, ³J = 3.0 Hz, ⁴J = 0.3 Hz, CHN¹), 8.48 (dd, 2H, ³J = 2.6 Hz, ⁴J = 0.2 Hz, CHN³). ³¹C NMR [150 MHz, (CD₃)₂SO, δ_C] 26.7 (s, NCH₂CH₂), 46.7 (s, NCH₂), 118.8 (t, J_{CF} = 53.2 Hz, *ipso*-C₆F₅), 121.0 (s, CHN¹), 128.2 (s, CHN³), 136.0 (dm, J_{CF} = 249.8 Hz, *para*-C₆F₅), 137.4 (dm, J_{CF} = 243.9 Hz, *meta*-C₆F₅), 139.7 (s, NC(H)N), 148.6 (ddm, J_{CF} = 228.6 Hz, J_{CF} = 23.8 Hz, *ortho*-C₆F₅). ¹⁵N NMR [61 MHz, (CD₃)₂SO, δ_N] –168.4 (s, N3), –200.7 (s, N1). ¹⁹F NMR [376 MHz, (CD₃)₂SO, δ_F] –116.2 (m, 2F, *ortho*-F), –161.3 (t, J_{FF} = 21.2 Hz, 2F, *meta*-F), –164.0 (m,

F, *para*-F). Anal. Calc. for C₂₂H₁₄N₄F₁₀Au₂ (918.30): C, 28.78; H, 1.54; N, 6.10. Found: C, 28.86; H, 1.51; N, 6.15%.

4.7. Preparation of [2,2-bis(4,5-dimethylthiazol-2-yl)](pentafluorophenyl)gold(I) (**6**)

The addition of a solution of 2,2'-bis(4,5-dimethylthiazole) (0.03 g, 0.20 mmol) in diethyl ether (10 ml) to [Au(C₆F₅)(tht)] (0.14 g, 0.30 mmol) in diethyl ether (10 ml), produced an immediate thick precipitate. The resultant suspension was stirred at room temperature for 1 h, filtered and washed sequentially with diethyl ether (10 ml) and dichloromethane (10 ml), to afford a highly insoluble off-white microcrystalline material of **6** (0.08 g). Repeating the reaction with equimolar amounts of [Au(C₆F₅)(tht)] and the bithiazole effected the same result. Crystals of suitable dimension were obtained by layering a solution of [Au(C₆F₅)(tht)] (0.02 mg, 0.03 mmol) in thf (1 ml) in a crystallisation tube with diethyl ether (1 ml) followed by a solution of bithiazole (0.01 g, 0.03 mmol) in *n*-pentane (1 ml). Leaving the reaction at –20 °C, the first crystalline product formed within hours at the contact point between the reagent solutions.

Yield: 93%. Mp: 182 °C (decomp.). EI-MS, *m/z* (relative intensity) for C₁₆H₁₂AuF₅N₂S₂: 588 (M⁺, 21), 334 (C₁₂F₁₀⁺, 37), 265 (C₁₂F₁₀⁺–CF₃, 16), 224 (M⁺–AuC₆F₅, 100). Anal. Calc. for C₁₆H₁₂AuF₅N₂S₂ (588.36): C, 32.66; H, 2.06; N, 4.76. Found: C, 32.78; H, 2.09; N, 4.91%.

4.8. Preparation of 1-benzyltetrazole(pentafluorophenyl)gold(I) (**7**)

This product was prepared in a similar manner as **1** from 1-benzyltetrazole (0.39 g, 2.4 mmol) and [Au(C₆F₅)(tht)] (1.1 g,

Table 4
Crystallographic data.

	6	7-C₈H₈N₄
Empirical formula	C ₁₆ H ₁₂ F ₅ N ₂ S ₂ Au	C ₂₂ H ₁₆ F ₅ N ₈ Au
<i>M_r</i>	588.36	684.38
<i>T</i> (K)	100(2)	100(2)
λ (Å)	0.71073	0.71073
Crystal system	triclinic	monoclinic
Space group	<i>P</i> $\bar{1}$	<i>P</i> 2 ₁ / <i>c</i>
<i>a</i> (Å)	6.875(4)	18.4500(13)
<i>b</i> (Å)	11.536(6)	5.0734(4)
<i>c</i> (Å)	11.747(6)	25.1579(17)
α (°)	112.809(7)	90
β (°)	94.191(8)	107.5310(10)
γ (°)	99.105(8)	90
<i>V</i> (Å ³)	838.7(8)	2245.5(3)
<i>Z</i>	2	4
<i>D</i> _{calc} (g cm ⁻³)	2.330	2.024
Absorption coefficient (μ , mm ⁻¹)	9.074	6.623
Absorption correction	semi-empirical from equivalents	semi-empirical from equivalents
<i>F</i> (000)	556	1312
Crystal size (mm)	0.30 × 0.10 × 0.05	0.20 × 0.10 × 0.10
θ -range for data collection (°)	1.90–25.68	1.70–26.73
Index range	–8 ≤ <i>h</i> ≤ 8 –7 ≤ <i>k</i> ≤ 14 –14 ≤ <i>l</i> ≤ 14	–23 ≤ <i>h</i> ≤ 22 –6 ≤ <i>k</i> ≤ 6 –26 ≤ <i>l</i> ≤ 31
Number of reflections collected	4412	12484
Number of independent reflections	3081 (<i>R</i> _{int} = 0.0277)	4727 (<i>R</i> _{int} = 0.0404)
Maximum and minimum transmission	0.6597 and 0.2428	0.5572 and 0.4477
Refinement method	Full-matrix least-squares on <i>F</i> ²	Full-matrix least-squares on <i>F</i> ²
Data/restraints/parameters	3081/0/239	4727/0/325
Gof on <i>F</i> ²	1.064	1.057
Final <i>R</i> -indices [<i>I</i> > 2 σ (<i>I</i>)]	<i>R</i> ₁ = 0.0355 <i>wR</i> ₂ = 0.0909	<i>R</i> ₁ = 0.0391 <i>wR</i> ₂ = 0.0851
<i>R</i> indices (all data)	<i>R</i> ₁ = 0.0393 <i>wR</i> ₂ = 0.0931	<i>R</i> ₁ = 0.0502 <i>wR</i> ₂ = 0.0894
Largest difference in peak and hole (e Å ⁻³)	3.027 and –2.290	2.977 and –1.524
Weighing scheme	<i>a</i> = 0.0586	<i>a</i> = 0.0490

2.4 mmol). An *n*-hexane extract of the dried product residue, was recrystallised and afforded colourless crystals of **7** (0.79 g), from a dichloromethane solution layered with diethyl ether, at –20 °C.

Yield: 62%. Mp: 121 °C (decomp.). EI-MS, *m/z* (relative intensity) for C₁₄H₈AuF₅N₄: 524 (M⁺, 3), 364 (AuC₆F₅⁺, 3), 334 (C₁₂F₁₀⁺, 100), 265 (C₁₁F₇⁺, 40). ¹H NMR [300 MHz, (CD₃)₂CO, δ_{H}] 5.80 (s, 2H, CH₂Ph), 7.40–7.46 (m, 5H, C₆H₅), 9.24 (s, 1H, NC(H)N). ¹³C NMR [75 MHz, (CD₃)₂CO, δ_{C}] 53.2 (s, NCH₂), 118.7 (tm, *J*_{CF} = 56.8 Hz, *ipso*-C₆F₅), 130.5 (s, *meta*-C₆H₅CH₂), 130.8 (s, *para*-C₆H₅CH₂), 131.2 (s, *ortho*-C₆H₅CH₂), 137.2 (s, *ipso*-C₆H₅CH₂), 141.3 (dm, *J*_{CF} = 250.7 Hz, *para*-C₆F₅), 139.9 (dm, *J*_{CF} = 245.4 Hz, *meta*-C₆F₅), 145.6 (s, NC(H)N), 150.1 (ddm, *J*_{CF} = 223.9 Hz, *J*_{CF} = 26.9 Hz, *ortho*-C₆F₅). ¹⁵N NMR [61 MHz, (CD₃)₂CO, δ_{N}] –9.0 (s, N³), –37.0 (s, N⁴), –50.2 (s, N²), –141.2 (s, N¹). Anal. Calc. for C₁₄H₈AuF₅N₄ (524.20): C, 32.08; H, 1.54; N, 10.69. Found: C, 32.24; H, 1.51; N, 10.78%.

4.9. Preparation of (trimethylphosphine)(tetrazol-1-yl)gold(I) (**VII**)

This product was prepared in a similar manner as **VI** [25] from [AuCl(PMe₃)] (0.56 g, 1.8 mmol) and 1-*H* tetrazole (0.13 g, 1.8 mmol) in acetone (60 ml), treated with 1.0 M aqueous NaOH (1.8 ml, 1.8 mmol). Colourless microcrystalline material of **VII** (0.46 g) was obtained, from a methanol solution layered with *n*-pentane, at –20 °C.

Yield: 74%. Mp: 154 °C (decomp.). FAB-MS, *m/z* (relative intensity) for C₄H₁₀AuN₄P: 349 (Au(PMe₃)₂⁺, 15), 342 (M⁺, 72), 314 (M⁺–N₂, 4), 273 ({M⁺–CHN₄}, 100). ¹H NMR [300 MHz, (CD₃)₂SO, δ_{H}] 0.87 (d, 9H, ¹*J* = 12.0 Hz, CH₃), 7.95 (s, 1H, CH). ¹³C NMR [75 MHz, (CD₃)₂SO, δ_{C}] 5.4 (d, ¹*J* = 42.1 Hz, CH₃), 140.7 (bs, CH). ³¹P NMR [61 MHz, (CD₃)₂SO, δ_{P}] –10.1 (s). Anal. Calc. for C₄H₁₀AuN₄P (342.09): C, 14.04; H, 2.95; N, 16.38. Found: C, 14.31; H, 2.72; N, 16.10%.

4.10. X-ray crystal structure determinations

Specimens of suitable quality and size of **1**, **2**, **3**, **4**-CH₂Cl₂, **6** and **7**-C₈H₈N₄ were mounted on the ends of glass fibres in inert oil and used for intensity data collection on a Bruker SMART Apex CCD diffractometer [34], employing graphite-monochromated Mo *K* α radiation (λ = 0.71073 Å). Data reduction was carried out using the SAINT [35] suite of programs and multi-scan absorption corrections were performed with SADABS [36,37].

The structures were solved by a combination of direct methods (SHELXS-97) and difference-Fourier syntheses and refined by full matrix least-squares calculations on *F*² (SHELXL-97) [38] within the X-seed environment [39]. The thermal motion was treated anisotropically for all non-hydrogen atoms. All hydrogen atoms were calculated in ideal positions and refined using a riding model. Further details regarding the data collection and structure refinement for compounds **1**, **2**, **3**, **4**-CH₂Cl₂, **6** and **7**-C₈H₈N₄ are listed in Tables 2–4. Figures were generated with X-seed [39] and POV Ray for Windows, with the displacement ellipsoids at 50% probability level.

4.11. Biological assays

4.11.1. Formulation of drugs

Cisplatin was included as a control for comparison. Ten millimolar stock solutions of the experimental compounds in DMSO were prepared (concentration ≤0.1%). Further dilutions were made in the appropriate tissue culture medium which was supplemented with 10% heat-inactivated, foetal calf serum (FCS) just before use.

4.11.2. Cell lines and culture conditions

The human cervical carcinoma (HeLa, ATCC No. CCL2) cell line – adherent epithelial cells maintained in Eagles minimum essential

medium (EMEM) containing 2 mM L-glutamine, 0.1 mM non-essential amino acids, 1.0 mM sodium pyruvate and 5% bovine FCS – were used.

To determine the tumour specificity of **1**, **VI** and cisplatin the non-cancerous cell culture, primary human lymphocytes, isolated as described by Anderson et al. [40], from heparinised human blood, obtained from healthy volunteers, was used. Cell suspensions were prepared using Histopaque-1077 (Sigma–Aldrich, St. Louis, MO, USA) as described by Smit et al. [41]. The cells were maintained in RPMI medium. The bovine FCS that was used to supplement the growth media was heat inactivated at 56 °C for 30 min. All the cultures were cultivated in the presence of 1% penicillin and streptomycin and were maintained at 37 °C with 5% CO₂. Cultures were sub-cultured as needed.

4.11.3. Cytotoxicity assays

Cytotoxicity assays were performed to establish the sensitivity of cancer cell lines and normal cell cultures to the experimental compounds. 5×10^2 cells/well were exposed to different concentrations (0.5–50 μM) of the complexes in 96-well tissue culture plates and incubated in a 5% CO₂ incubator for 7 days at 37 °C. Drug-free solvent controls were included. The IC₅₀ data for cisplatin were determined under the same conditions. Dose–response assays were performed to derive IC₅₀ values against resting and phytohaemagglutinin (PHA)-stimulated human lymphocytes in order to determine whether cytotoxicity observed against HeLa cells may not be tumour specific. The final concentration of PHA that was added to the relevant wells was 5 μg/ml. Cancer cells were seeded at $4\text{--}5 \times 10^2$ /well and were incubated for 7 days. Lymphocytes were seeded at 2×10^5 /well and incubated for 3 days. The viability of cells was determined with an MTT assay [42] originally described by Mosmann [43] with modifications by van Rensburg et al. [44]. A volume of 20 μl MTT [3-(4,5-dimethylthiazol-2-yl)-2,5-diphenyltetrazolium bromide] (Sigma Diagnostics Inc.) was added to each well. MTT is a pale yellow substance that is metabolized to dark blue formazan crystals by unaffected metabolically active cells, which is then quantified by means of spectrometry. The same method was used for both cancer cells and normal cell lines. A minimum of three independent experiments were performed where the availability of the test compounds allowed. Data were processed using a Wilcoxon signed-rank test at a confidence interval of 95% and with GRAPHAD Prism 4 software©.

Acknowledgements

We gratefully thank the Alexander von Humboldt Stiftung (H.G.R., S.C., S.N.) and the NRF (National Research Foundation, South Africa) for financial support and Harmony Gold Mining Co. Ltd. (WFG), through Mintek (Project Autek), for the generous loan of gold.

Appendix A. Supplementary data

CCDC 847311, 847312, 847313, 847314, 847315 contain the supplementary crystallographic data for **1**, **2**, **3**, **4-CH₂Cl₂**, **6** and **7-C₈H₈N₄**, respectively. These data can be obtained free of charge via <http://www.ccdc.cam.ac.uk/conts/retrieving.html>, or from the Cambridge Crystallographic Data Centre, 12 Union Road, Cambridge CB2 1EZ, UK; fax: (+44) 1223-336-033; or e-mail: deposit@ccdc.cam.ac.uk.

References

- [1] M.C. Gimero, A. Laguna, in: J.A. McCleverty, T.J. Meyer, D.E. Fenton (Eds.), *Comprehensive Coordination Chemistry II*, vol. 6, Elsevier, Amsterdam, 2004, p. 911.
- [2] J. Coetzee, S. Cronje, L. Dobrzańska, H.G. Raubenheimer, M.J. Nell, G. Jooné, H. Hoppe, *Dalton Trans.* 40 (2011) 1471.
- [3] (a) U.E.I. Horvath, S. Cronje, J.M. McKenzie, L.J. Barbour, H.G. Raubenheimer, *Z. Naturforsch.* 59b (2004) 1605, and references therein; (b) Also: U.E.I. Horvath, H.G. Raubenheimer, unpublished results.
- [4] J.R. Lechat, R.H. De Almeida-Santos, G. Banditelli, F. Bonati, *Cryst. Struct. Commun.* 11 (1982) 471.
- [5] F. Bonati, A. Burini, B.R. Pietroni, E. Georgini, *J. Organomet. Chem.* 344 (1988) 119.
- [6] F. Bachechi, A. Burini, R. Galassi, B.R. Pietroni, M. Severini, *J. Organomet. Chem.* 575 (1999) 269.
- [7] F. Bachechi, A. Burini, R. Galassi, B.R. Pietroni, D. Tesei, *Z. Kristallogr.* 214 (1999) 497.
- [8] D. Leonesi, A. Lorenzotti, A. Cingolani, F. Bonati, *Gazz. Chim. Ital.* 111 (1981) 483.
- [9] D. Matovič, D.J. Radanović, G. Ponticelli, P. Scano, I.A. Efimenko, *Transition Met. Chem.* 19 (1994) 461.
- [10] S. Cronje, H.G. Raubenheimer, H.S.C. Spies, C. Esterhuysen, H. Schmidbaur, A. Schier, G.J. Kruger, *Dalton Trans.* 14 (2003) 2859.
- [11] E.R.T. Tiekink, *Inflammopharmacology* 16 (2008) 138, and references therein.
- [12] S. Nobili, E. Mini, I. Landini, C. Gabbiani, A. Casini, L. Messori, *Med. Res. Rev.* 30 (2010) 550, and references therein.
- [13] E. Vergara, E. Cerrada, A. Casini, O. Zava, M. Laguna, P.J. Dyson, *Organometallics* 29 (2010) 2596, and references therein.
- [14] E.R.T. Tiekink, *Crit. Rev. Oncol./Hematol.* 42 (2002) 225.
- [15] P.J. Barnard, S.J. Berners-Price, *Coord. Chem. Rev.* 251 (2007) 1889, and references therein.
- [16] C.K. Mirabelli, D.T. Hill, L.F. Faucette, F.L. McCabe, G.R. Girard, D.B. Byran, B.M. Sutton, J. O'Leary Bartus, S.T. Crooke, R.K. Johnson, *J. Med. Chem.* 30 (1987) 2181.
- [17] K. Spiegel, A. Magistrato, P. Carloni, J. Reedijk, M.L. Kelin, *J. Phys. Chem. B* 111 (2007) 11873.
- [18] U.E.I. Horvath, G. Bentivoglio, M. Hummel, H. Schottenberger, K. Wurst, M.J. Nell, C.E. Janse van Rensburg, S. Cronje, H.G. Raubenheimer, *New J. Chem.* 32 (2008) 533.
- [19] A. Luquin, E. Cerrada, M. Laguna, in: F. Mohr (Ed.), *Gold Chemistry: Applications and Future Directions in the Life Sciences*, Wiley-VCH Verlag, Weinheim, Germany, 2009, p. 93; (b) J. Coetzee, W.F. Gabrielli, K. Coetzee, O. Schuster, S.D. Nogai, S. Cronje, H.G. Raubenheimer, *Angew. Chem., Int. Ed.* 46 (2007) 2497.
- [20] A. Burini, B.R. Pietroni, R. Galassi, G. Valke, S. Cologero, *Inorg. Chim. Acta* 229 (1995) 299.
- [21] (a) E. Takach, R.H. Henry, D.W. Moore, W.M. Tolles, G.A. Gray, *Magn. Res. Chem.* 24 (1986) 984; (b) M. Forkey, W.R. Carpenter, *Org. Mass Spectrosc.* 2 (1969) 433; (c) W.F. Gabrielli, S.D. Nogai, J.M. McKenzie, S. Cronje, H.G. Raubenheimer, *New J. Chem.* 33 (2009) 2208.
- [22] (a) H. Schmidbaur, A. Wohlleben, F.E. Wagner, D.F. Van de Vondel, G.P. Van der Kelen, *Chem. Ber.* 110 (1977) 2758; (b) P. Pyykkö, *Chem. Soc. Rev.* 37 (2008) 1967; (c) H. Schmidbaur, A. Schier, *Chem. Soc. Rev.* 41 (2012) 370.
- [23] V.J. Catalano, S.J. Horner, *Inorg. Chem.* 42 (2003) 8430.
- [24] K. Nomiyama, R. Noguchi, M. Oda, *Inorg. Chim. Acta* 298 (2000) 24.
- [25] R.L. Kieft, W.M. Peterson, G.L. Blundell, S. Horton, R.A. Henry, H.B. Jonassen, *Inorg. Chem.* 15 (1976) 1721.
- [26] P.J. Barnard, L.E. Wedlock, M.V. Baker, S.J. Berners-Price, D.A. Joyce, B.W. Skelton, J.A. Steer, *Angew. Chem., Int. Ed.* 45 (2006) 5966, and references therein.
- [27] Y. Satoh, N. Marcopulos, *Tetrahedron Lett.* 36 (1995) 1759.
- [28] L.J. Mathias, D. Burkett, *Tetrahedron Lett.* 49 (1979) 4709.
- [29] J.-F. Ma, J. Yang, G.-L. Zheng, L. Li, J.-F. Liu, *Inorg. Chem.* 42 (2003) 7531.
- [30] R. Bronisz, *Inorg. Chim. Acta* 340 (2002) 215.
- [31] R. Mostaghim, Y.A. Beni, *Indian J. Chem.* 40B (2001) 498.
- [32] R. Usòn, A. Laguna, in: R.B. Lang, J.J. Eisch (Eds.), *Organometallic Synthesis*, vol. 3, Elsevier, Amsterdam, 1986, p. 325.
- [33] R. Usòn, A. Laguna, in: R.B. Lang, J.J. Eisch (Eds.), *Organometallic Synthesis*, vol. 3, Elsevier, Amsterdam, 1986, p. 326.
- [34] SMART Data Collection Software, Version 5.629, Bruker AXS Inc., Madison, WI, 2003.
- [35] SAINT, Data Reduction Software, Version 6.45, Bruker AXS Inc., Madison, WI, 2003.
- [36] R.H. Blessing, *Acta Crystallogr., Sect. A* 51 (1995) 33.
- [37] SADABS, Version 2.05, Bruker AXS Inc., Madison, WI, 2002.
- [38] G.M. Shelrick, *SHELX-97*. Program for Crystal Structure Analysis, University of Göttingen, Germany, 1997.
- [39] L.J. Barbour, *J. Supramol. Chem.* 1 (2001) 189.
- [40] R. Anderson, M.J. Smit, C.E. Janse van Rensburg, *Mol. Pharmacol.* 44 (1993) 605.
- [41] T. Smit, J.R. Snyman, E.W. Neuse, L. Bohm, C.E. Janse van Rensburg, *Anti-Cancer Drug* 16 (2005) 501.
- [42] G.D. Hoke, G.F. Rush, G.E. Bossard, J.V. McArdle, B.D. Jensen, C.K. Mirabelli, *J. Biol. Chem.* 263 (1988) 11203.
- [43] T. Mosmann, *J. Immunol. Meth.* 65 (1983) 55.
- [44] C.E. Janse van Rensburg, R. Anderson, G. Joone, M.S. Myer, J.F. O'Sullivan, *Anti-Cancer Drug* 8 (1997) 708.